RNA (2000), *6*:1056–1068. Cambridge University Press. Printed in the USA.

The human coronavirus 229E superfamily 1 helicase has RNA and DNA duplex-unwinding activities with 5′-to-3′ polarity

ANJA SEYBERT, ANNETTE HEGYI, STUART G. SIDDELL, and JOHN ZIEBUHR
Institute of Virology and Immunology, University of Würzburg, 97078 Würzburg, Germany

ABSTRACT

The human coronavirus 229E replicase gene encodes a protein, p66^{HEL}, that contains a putative zinc finger structure linked to a putative superfamily (SF) 1 helicase. A histidine-tagged form of this protein, HEL, was expressed using baculovirus vectors in insect cells. The purified recombinant protein had in vitro ATPase activity that was strongly stimulated by poly(U), poly(dT), poly(C), and poly(dA), but not by poly(G). The recombinant protein also had both RNA and DNA duplex-unwinding activities with 5′-to-3′ polarity. The DNA helicase activity of the enzyme preferentially unwound 5′-oligopyrimidine-tailed, partial-duplex substrates and required a tail length of at least 10 nucleotides for effective unwinding. The combined data suggest that the coronaviral SF1 helicase functionally differs from the previously characterized RNA virus SF2 helicases.

Keywords: 5′-to-3′ polarity; helicase; nucleoside triphosphatase; superfamily 1

INTRODUCTION

RNA helicases are a diverse class of enzymes that use the energy of nucleoside triphosphate (NTP) hydrolysis to unwind duplex RNA. They are involved in virtually every aspect of RNA metabolism, including transcription, splicing, translation, export, ribosome biogenesis, mitochondrial gene expression, and the regulation of mRNA stability (Schmid & Linder, 1992; Lohman & Bjornson, 1996; de la Cruz et al., 1999; Linder & Daugeron, 2000). On the basis of conserved sequence motifs, and the arrangement of these motifs, both RNA and DNA helicases have been divided into three large superfamilies and two smaller families. The superfamilies are called SF1, SF2, and SF3 (Gorbalenya et al., 1989b; Gorbalenya & Koonin, 1993).

More than a decade ago, nearly all double-stranded and positive-stranded (+) RNA viruses were predicted to encode putative helicases (Gorbalenya & Koonin, 1989). Indeed, apart from the RNA-dependent RNA polymerases (RdRp), they are the most conserved subunits of the RNA virus replication machinery (Koonin & Dolja, 1993). Also, there is extensive genetic evidence to suggest a key function for helicases in the life-cycle of (+) RNA viruses (for reviews, see Buck, 1996; Kadaré & Haenni, 1997). However, despite their importance, the reactions catalyzed by (+) RNA virus-encoded helicases have not been well defined and their precise role in virus replication is poorly understood. Thus, for example, from the large group of putative RNA virus-encoded helicases, only members of SF2 have been associated with duplex-unwinding activity. In this respect, the hepatitis C virus NS3 (HCV NS3) protein is the best-characterized enzyme. Structural analyses using X-ray crystallography (Yao et al., 1997; Cho et al., 1998; Kim et al., 1998) have shown that HCV NS3 is structurally related to the *Bacillus stearothermophilus* PcrA and *Escherichia coli* Rep SF1 DNA helicases. All three enzymes share two subdomains, 1A and 2A, that represent an internal repeat of RecA-like subdomains (Subramanya et al., 1996; Korolev et al., 1997; Yao et al., 1997; Velankar et al., 1999). Also, it is increasingly clear that the 1A and 2A subdomains, which represent the "core helicase," may be decorated with additional domains to produce specific enzymatic activities (Bird et al., 1998; Korolev et al., 1998). The biochemical characterization of HCV NS3, together with other RNA virus-encoded SF2 enzymes, has revealed that these proteins share a 3′-to-5′ polarity in their unwinding activities (for reviews, see Kadaré & Haenni, 1997; Kwong et al., 2000).

Reprint requests to: John Ziebuhr, Institute of Virology and Immunology, University of Würzburg, Versbacher Str. 7, 97078 Würzburg, Germany; e-mail: ziebuhr@vim.uni-wuerzburg.de.

The majority of putative RNA virus helicases has been classified as belonging to SF1 (Gorbalenya & Koonin, 1989; Kadaré & Haenni, 1997). This group includes proteins from a variety of plant virus families, as well as alphaviruses, rubiviruses, hepatitis E viruses, arteriviruses, and coronaviruses. Biochemical and genetic data clearly implicate these proteins in diverse aspects of transcription, replication, RNA stability, cell-to-cell movement, and, most likely, even virus biogenesis (Kroner et al., 1990; Petty et al., 1990; Rouleau et al., 1994; O'Reilly et al., 1995, 1998; Dé et al., 1996; Osman & Buck, 1996; van Dinten et al., 1997, 1999; Janda & Ahlquist, 1998). However, to date, there is very little detailed information on the enzymatic properties of RNA virus SF1 helicases. Specifically, attempts to detect convincing duplex-unwinding activities have been essentially unsuccessful (Kadaré & Haenni, 1997). In a few cases, the proteins have been shown to have NTPase activities but, in striking contrast to other helicases, these activities were not significantly stimulated by homopolynucleotides (Rikkonen et al., 1994; Gros & Wengler, 1996; Kadaré et al., 1996; Heusipp et al., 1997). Therefore, the designation of RNA virus SF1 (and also SF3) helicase proteins as enzymes with nucleic acid-unwinding activities has been increasingly questioned (Rodriguez & Carrasco, 1993; Kadaré & Haenni, 1997; Pfister & Wimmer, 1999).

Putative SF1 RNA helicase domains have been identified in the replicase gene products of coronaviruses (Gorbalenya et al., 1989a). In the case of the human coronavirus 229E (HCoV), the helicase motifs reside in a protein of 597 amino acids called $p66^{HEL}$. This protein is processed from the replicase polyprotein, pp1ab, by the virus-encoded 3C-like proteinase (Ziebuhr et al., 1995, 2000; Heusipp et al., 1997). Sequence analyses and immunoprecipitation data suggest that the coronavirus helicase protein, in common with the closely related arterivirus helicase protein, nsp10 (den Boon et al., 1991; van Dinten et al., 1996), differs from most other RNA virus helicases in at least two important respects. First, the coronavirus helicase domain is linked at its amino terminus to a putative zinc finger structure in a single protein (Gorbalenya et al., 1989a). Second, the helicase domain occupies a position in the viral polyprotein downstream of the RdRp. This arrangement is unique among positive-stranded RNA viruses where the helicase protein generally precedes RdRp in the viral polyprotein (Koonin & Dolja, 1993).

We show here that the putative HCoV SF1 helicase has both RNA and DNA energy-dependent duplex-unwinding activities. We found that sequence variation in the 5′ single-stranded regions of partial-duplex substrates affected duplex-unwinding activity and, importantly, we show that the coronavirus helicase activity has a 5′-to-3′ polarity. Our experimental data support previous sequence-based predictions and indicate that the coronavirus SF1 helicase differs significantly from RNA virus helicases of SF2.

RESULTS

Expression and purification of the recombinant HCoV helicase protein, HEL

We have used the baculovirus expression system to obtain sufficient amounts of the HCoV helicase for biochemical studies. First, we produced a recombinant baculovirus, vBac-Hel, that encodes the HCoV helicase protein (pp1ab amino acids 4998–5592) fused at the amino terminus to 32 vector-derived amino acids, including 6 consecutive His residues and an enterokinase cleavage site. This protein was designated HEL. Second, we produced a recombinant baculovirus that encodes a similar protein in which the Lys residue (pp1ab amino acid 5284) of the Walker A motif (Walker et al., 1982) was substituted by Ala. This protein was designated HEL-KA. The high-affinity binding of the His-tagged proteins to nickel-charged agarose was used to purify the recombinant proteins to near homogeneity (Fig. 1A). Routinely, we obtained approximately 45 μg of HEL and 2100 μg of HEL-KA from 10^8 baculovirus-infected cells. We consistently found that the expression level of HEL was about 45-fold lower than that of HEL-KA (data not shown). We believe that the observed difference might result from toxic effects of the HEL-associated enzymatic activities on the host cell.

The identity of the recombinant proteins was confirmed by western blot analysis using the HCoV helicase-specific monoclonal antibody (mab) 6.2.E11. As shown in Figure 1B, no specific reaction was detected in lysates from mock-infected cells. However, in vBac-Hel-infected cells, we detected a protein with a migration in SDS gels corresponding to the calculated molecular mass of HEL (70 kDa). After purification, both of the purified recombinant proteins reacted specifically with mab 6.2.E11 (Fig. 1B).

Attempts to remove the amino-terminal fusion polypeptide from the purified proteins by enterokinase treatment failed. Even after prolonged incubation with this endopeptidase at 25 °C, only a minor proportion of the recombinant proteins was cleaved (data not shown). However, because the ATPase activity of $p66^{HEL}$ has been shown to tolerate an amino-terminal fusion to the *E. coli* maltose-binding protein (MBP) (Heusipp et al., 1997), we decided to use the His-tagged protein in the experiments reported here.

Stimulation of the HEL protein-associated NTPase activity by nucleic acids

Stimulation of the NTPase activity by nucleic acids is an intrinsic property of most helicases (Lohman & Bjornson, 1996). In this study, we examined the effect of

https://doi.org/10.1017/S1355838200000728 Published online by Cambridge University Press

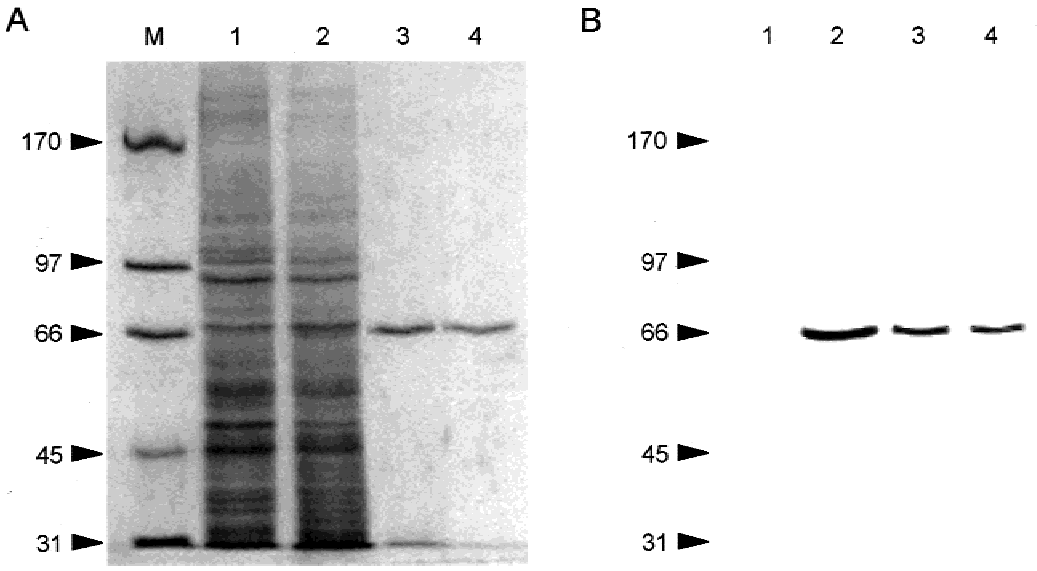

FIGURE 1. Purification of HEL and HEL-KA from extracts of High Five™ insect cells infected with recombinant baculoviruses. His-tagged recombinant proteins were purified by affinity chromatography as described in Materials and methods. **A**: An SDS-10% polyacrylamide gel stained with Coomassie brilliant blue dye. Lane M: protein molecular mass markers (with masses, in kilodaltons, indicated on the left); lane 1: total cell lysate from 1.5×10^4 mock-infected cells; lane 2: total cell lysate from 1.5×10^4 cells infected with vBac-Hel; lane 3: 500 ng of purified HEL protein; lane 4: 400 ng of purified HEL-KA protein. **B**: Western immunoblot analysis using antibody 6.2.E11. Lane 1: total cell lysate from 1.5×10^4 mock-infected cells; lane 2: total cell lysate from 1.5×10^4 cells infected with vBac-Hel; lane 3: 60 ng of purified HEL protein; lane 4: 50 ng of purified HEL-KA protein. The mobility of dye-stained protein molecular mass markers (with masses, in kilodaltons) is indicated.

different DNA and RNA polynucleotides on ATP hydrolysis by the recombinant HCoV HEL protein. First, we analyzed the activity of HEL in ATPase and GTPase assays. In these experiments, we were able to demonstrate hydrolysis of both ATP and GTP by HEL (data not shown), a result that essentially confirms our earlier studies with an MBP-p66^{HEL} fusion protein (Heusipp et al., 1997). In contrast, the activity of HEL-KA protein was $\leq$1% of the wild-type activity in both assays, supporting the indispensability of Lys-5284 for the NTPase activity of the HCoV helicase domain. This result is consistent with previous mutagenesis studies that have implicated equivalent Lys residues of the Walker A motif in the function of numerous helicase-associated ATPase activities (reviewed in Hall & Matson, 1999). The results also strongly suggest that the observed NTPase activity is mediated by HEL rather than any minor impurity and that HEL-KA would be an appropriate negative control in subsequent experiments.

Next, we compared the stimulatory effects of different polynucleotides on the ATPase activity of HEL (Table 1). The extent of ATP hydrolysis without added polynucleotides was determined after 30 min and taken to be 1.0. All other activity values were normalized to this value. Also, the enzyme concentration was adjusted to give substrate hydrolysis of not more than 20%. The data show that poly(U), poly(dT), poly(dA), and poly(C) are the strongest activators of the HEL-associated ATPase activity with a 32- to 50-fold increase of the basal ATPase activity. In the presence of poly(U), which proved to be the best cofactor, 1 pmol HEL hydrolyzed 7 nmol ATP per minute. Similar specific activities have previously been reported for both the HCV NS3 protein (hydrolysis of 1.3 nmol ATP per pmol enzyme and minute; Suzich et al., 1993) and the vaccinia virus NPH-II helicase (Gross & Shuman, 1995). Poly(A) was found to stimulate the ATPase activity of HEL to a lesser extent and poly(G) and tRNA were essentially inactive. The data show that the ATPase activity of HEL is strongly stimulated by specific single-stranded nucleic acids. It should be noted that this result stands in sharp contrast to all other RNA virus SF1

TABLE 1. Effect of polynucleotides on the ATPase activity of HEL.

Polynucleotide	Relative ATPase activity[a]
None	1
Poly(U)	50
Poly(A)	5
Poly(C)	32
Poly(G)	1
Poly(dT)	47
Poly(dA)	48
tRNA	2

[a]The enzymatic activity without added polynucleotides was taken to be 1.0, and all other activity values were normalized to this value (see text for details). Each value represents the average of three independent determinations, which did not vary by more than 20%.

https://doi.org/10.1017/S1355838200000728 Published online by Cambridge University Press

helicases studied to date, where stimulatory effects of not more than twofold have been reported (Rikkonen et al., 1994; Gros & Wengler, 1996; Kadaré et al., 1996).

RNA duplex-unwinding activity of the HEL protein

To investigate the RNA duplex-unwinding activity of HEL, a standard helicase assay (reviewed in Lohman & Bjornson, 1996; Kadaré & Haenni, 1997) using partially double-stranded RNA molecules was used. In a first set of experiments, substrates with 3′ single-stranded regions were used because, until now, all RNA virus-encoded helicases have been shown to unwind double-stranded substrates in the 3′-to-5′ direction. However, the data we obtained clearly show that HEL was not active on a substrate containing 3′ single-stranded tails (113- and 203-nt single-stranded regions, 26-bp duplex region) (Fig. 2A). In contrast, the duplex substrate was unwound by HEL if it contained 5′ single-stranded tails (76-nt and 80-nt 5′ single-stranded regions, 33-bp duplex region) (Fig. 2B). Also, the duplex-unwinding activity required the presence of ATP (Fig. 2B, cf. lanes 3 and 4) or GTP (data not shown). This data is compatible with the current model of helicase activity where it is generally accepted that duplex-unwinding is an energy-dependent process in which the energy is derived from NTP binding and hydrolysis. In agreement with this model, the ATPase-deficient protein, HEL-KA, also lacked helicase activity (Fig. 2B, lane 5).

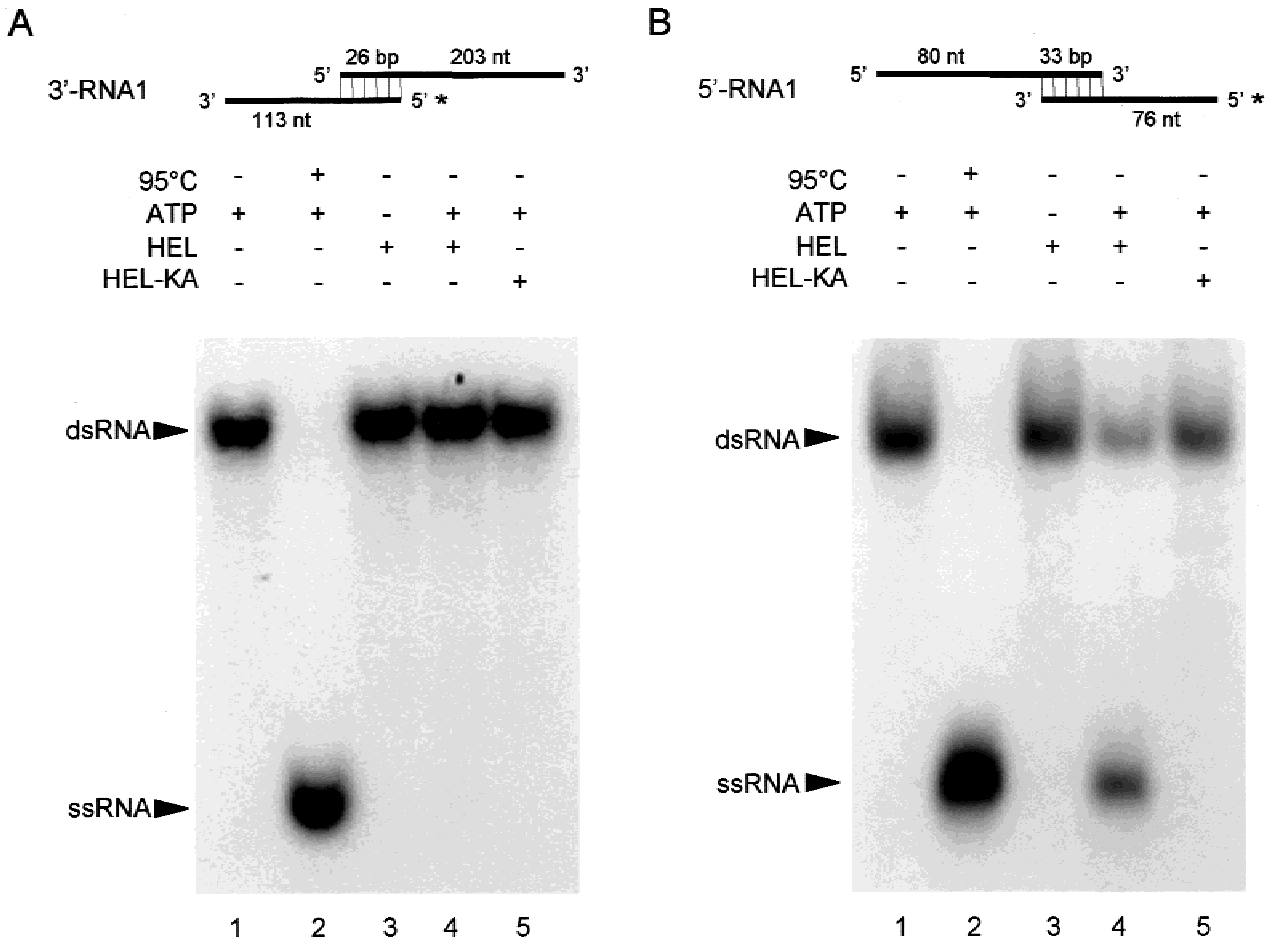

FIGURE 2. The RNA duplex-unwinding activity of HEL has 5′-to-3′ polarity. Reaction conditions were as described in Materials and methods with approximately 90 fmol of RNA substrates per reaction. The structures of the substrates are shown schematically with the radiolabeled strands marked by asterisks. The reaction products were separated on nondenaturing 6% polyacrylamide gels and visualized by autoradiography. The positions of the partially double-stranded substrates (dsRNA) and the displaced, monomeric products (ssRNA) are indicated. **A**: Helicase assay with substrate 3′-RNA1 containing 3′ single-stranded tails. Lane 1: reaction without protein; lane 2: heat-denatured RNA substrate; lane 3: reaction containing 300 fmol HEL in the absence of ATP; lane 4: reaction containing 300 fmol HEL in the presence of 5 mM ATP; lane 5: reaction containing 2.1 pmol HEL-KA in the presence of 5 mM ATP. **B**: Helicase assay with substrate 5′-RNA1 containing 5′ single-stranded tails. Lane 1: reaction without protein; lane 2: heat-denatured RNA substrate; lane 3: reaction containing 300 fmol HEL in the absence of ATP; lane 4: reaction containing 300 fmol HEL in the presence of 5 mM ATP; lane 5: reaction containing 2.1 pmol HEL-KA in the presence of 5 mM ATP.

https://doi.org/10.1017/S1355838200000728 Published online by Cambridge University Press

Next, we sought to exclude the possibility that different sequences present in the 3′ and 5′ overhangs of the substrates described above may have accounted for the inability of HEL to unwind the 3′-tailed substrate. Consequently, we tested substrates with similar sequences, essentially poly(U), in a 5′ or 3′ single-stranded region (Fig. 3). This analysis again revealed that HEL readily unwinds 5′-tailed duplex RNA (Fig. 3A, lane 3) but not 3′-tailed duplex RNA (Fig. 3B, lane 3). We interpret this data to show that HEL binds to the 5′ single-stranded region of a partial duplex RNA and unwinds the duplex RNA structure in a 5′-to-3′ direction with respect to the RNA strand that HEL is bound to.

DNA duplex-unwinding activity of the HEL protein

As described above, the ATPase activity of HEL is stimulated by some single-stranded DNA homopolymers. This result prompted us to analyze the unwinding activity of HEL on partial duplex DNA substrates. The substrates we used had identical, 22-bp DNA duplex regions to which 30-nt-long, single-stranded oligo(dT) tails were attached at different positions (Fig. 4). One substrate, DNA-0, contained no single-stranded region. The data shown in Figure 4 can be summarized as follows. Partial duplex DNA substrates with 5′ single-stranded tails alone or in combination with 3′ single-stranded tails (irrespective of whether they were present on the same end or the opposite end of the substrate) were readily unwound by HEL if a fourfold excess of enzyme over substrate was used (Fig. 4, lanes 7, 11, and 19). Complete unwinding was also observed with these substrates if equimolar amounts of enzyme and substrate were used (data not shown).

In contrast, if the DNA substrates contained only a 3′ tail or no single-stranded tail at all, duplex-unwinding did not occur (Fig. 4, lanes 3 and 15). The combined data indicate that the HEL-associated DNA duplex-unwinding activity depends on the presence of 5′ single-stranded regions in the duplex DNA substrate. This data is fully consistent with the RNA helicase activity

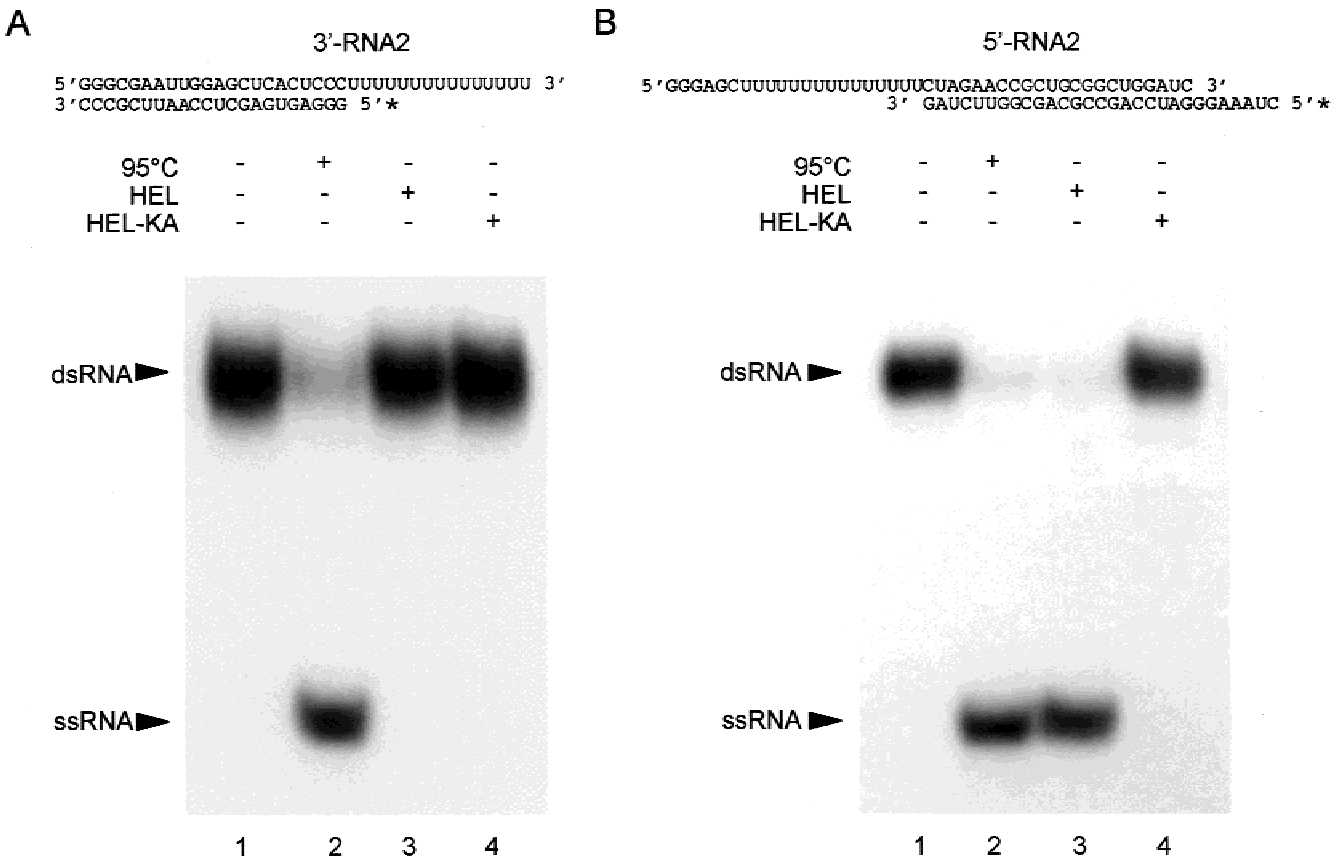

FIGURE 3. RNA duplex unwinding of HEL with substrates containing a 5′-oligo(U) tail. The experimental conditions were as described in Figure 2. **A**: Helicase assay with substrate 3′-RNA2 containing a 3′-oligo(U) tail. Lane 1: reaction without protein; lane 2: heat-denatured RNA substrate; lane 3: reaction containing 300 fmol HEL; lane 4: reaction containing 2.1 pmol HEL-KA. **B**: Helicase assay with substrate 5′-RNA2 containing oligo(U) in a 5′ single-stranded tail. Lane 1: reaction without protein; lane 2: heat-denatured RNA substrate; lane 3: reaction containing 300 fmol HEL; lane 4: reaction containing 2.1 pmol HEL-KA.

https://doi.org/10.1017/S1355838200000728 Published online by Cambridge University Press

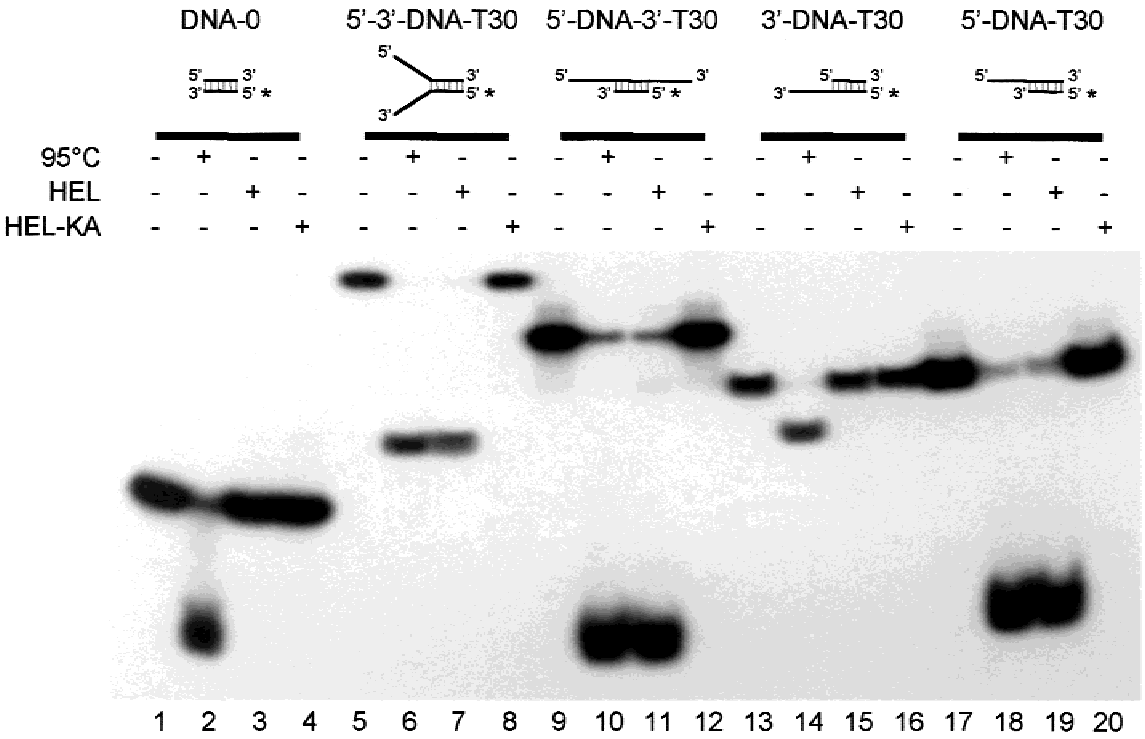

FIGURE 4. The DNA duplex-unwinding activity of HEL has 5′-to-3′ polarity. Reactions were done as described in Materials and Methods with approximately 25 fmol of DNA substrate per reaction and analyzed on nondenaturing, 10–20% gradient polyacrylamide gels. With the exception of DNA-0, which was entirely double-stranded, the substrates consisted of identical 22-bp duplexes to which 30-nt-long, single-stranded oligo(dT) tails were attached at different positions. Asterisks indicate radiolabeled strands. Lanes 1, 5, 9, 13, and 17: reactions without protein; lanes 2, 6, 10, 14, and 18: heat-denatured DNA substrates; lanes 3, 7, 11, 15, and 19: reactions containing 100 fmol HEL; lanes 4, 8, 12, 16, and 20: reactions containing 700 fmol HEL-KA.

described above and again supports the conclusion that the coronavirus helicase activity has 5′-to-3′ polarity.

Effect of substrate 5′-tail length and sequence on DNA duplex-unwinding activity of the HEL protein

The DNA duplex-unwinding activity of HEL provides a convenient system to characterize the coronavirus helicase in terms of substrate requirement, as it allows the use of substrates composed of synthetic oligonucleotides. First, we examined the effect of 5′ tail length on duplex-unwinding activity. In the experiment shown in Figure 5, 25 fmol of each of four substrates containing a 5′-oligo(dT) tail of 30, 20, 10, or 5 nt, attached to an identical 22-bp DNA duplex region, was incubated with 50 fmol of HEL. The results show that duplex-unwinding decreased only marginally as the 5′ tail was shortened from 30 to 10 nt (Fig. 5, lanes 3, 7, and 11) and a sharp decrease occurred at the transition from 10 to 5 nt (Fig. 5, lane 15). As before, no duplex-unwinding was observed if the substrate lacked a 5′ tail or if HEL-KA was used instead of HEL. We interpret these data to reflect a length requirement of about 10 nt for optimal binding of HEL to single-stranded DNA. Alternatively, it is conceivable that a tail of sufficient length is required for effective ATP hydrolysis.

We then determined the effect of the 5′-tail sequence on duplex-unwinding activity. This was done by comparing four 22-bp duplex DNA substrates, each of them containing a 10-nt-long 5′ tail consisting of either dA, dG, dC, or dT. In this experiment, shown in Figure 6, equal amounts of the four substrates (25 fmol) were unwound to different extents. The oligo(dT)- and oligo(dC)-tailed substrates were more readily unwound (Fig. 6, lanes 13 and 18), whereas substrates with oligo(dA) and oligo(dG) 5′ tails were less readily unwound (Fig. 6, lanes 3 and 8). The differences became even more obvious if low amounts of enzyme were used (Fig. 6, lanes 4, 9, 14, and 19). The results suggest that substrates with 5′-homodeoxypyrimidine tails are favored. One proviso that should be made is that, as is apparent in Figure 6, the poly(G)-tailed substrate we used tends to form high-molecular-weight structures. These structures most likely represent four-stranded helices that are known to be formed by stretches of guanine bases in the presence of sodium or potassium salts (Phillips et al., 1997). We cannot exclude that these structures interfere with the duplex-unwinding activity of the HEL protein.

https://doi.org/10.1017/S1355838200000728 Published online by Cambridge University Press

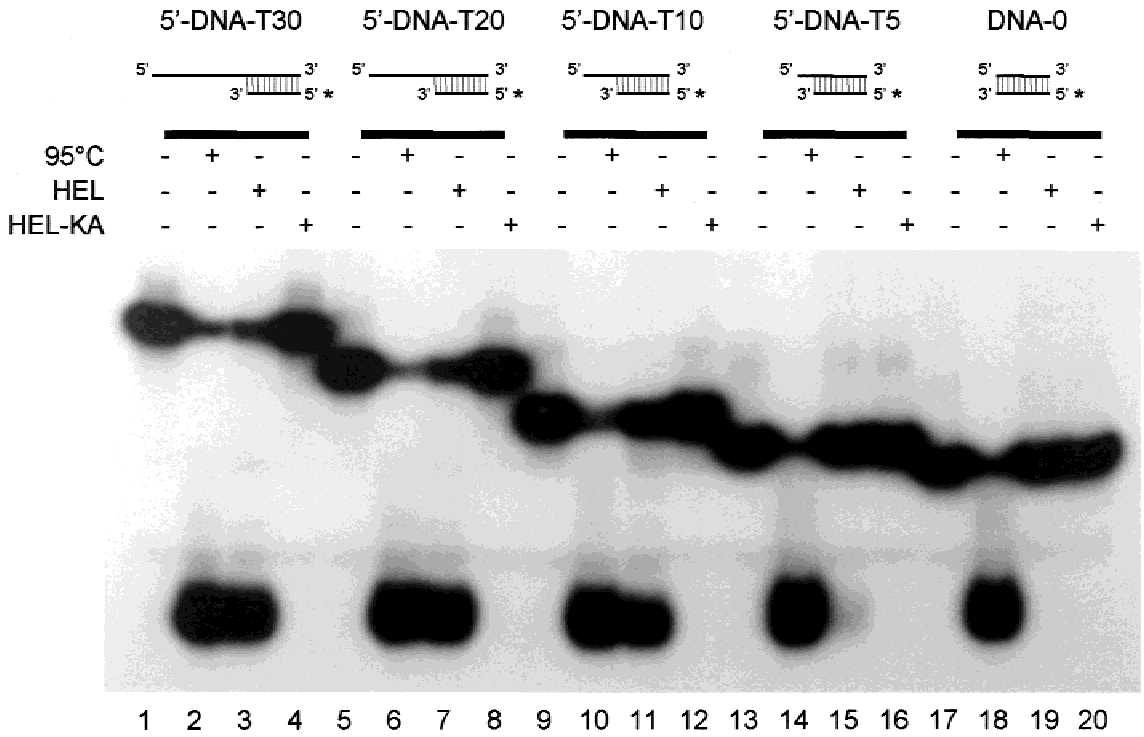

FIGURE 5. The effect of substrate 5′-tail length on DNA duplex unwinding activity of HEL. Reactions were done as described in Materials and methods with approximately 25 fmol of DNA substrate per reaction and analyzed on 10–20% gradient polyacrylamide gels. The DNA substrates consisted of identical 22-bp duplexes and varied by the length of the attached 5′-oligo(dT) tail. Asterisks indicate radiolabeled strands. Lanes 1, 5, 9, 13, and 17: reaction without protein; lanes 2, 6, 10, 14, and 18: heat-denatured DNA substrates; lanes 3, 7, 11, 15, and 19: reactions containing 50 fmol HEL; lanes 4, 8, 12, 16, and 20: reactions containing 350 fmol HEL-KA.

DISCUSSION

Identification of the HCoV SF1 RNA helicase activity

Sequence analyses have given rise to a wealth of predictions on the putative functions of virus-encoded proteins. Obviously, only a few of these predictions have been substantiated by experimental data. Moreover, in a number of cases, attempts to confirm the predicted activities have failed and the assignment of specific functions has then been called into doubt. This, in fact, is the case for a large family of related proteins of (+) RNA viruses that were predicted more than 10 years ago to be SF1 helicases (Gorbalenya & Koonin, 1989) but, so far, have not been shown to possess this activity (Kadaré & Haenni, 1997). Therefore, the RNA duplex-unwinding activity demonstrated here for the HCoV $p66^{HEL}$ protein settles a long debate on the correct identification of this class of viral enzymes as true helicases.

Biochemical properties of the HCoV helicase

In addition to establishing that HCoV $p66^{HEL}$ is an SF1 RNA helicase, we have shown that it differs significantly from the previously characterized SF2 RNA virus helicases. Thus, although all RNA virus helicases investigated so far operate in 3′-to-5′ direction (reviewed in Kadaré & Haenni, 1997), the coronavirus RNA duplex-unwinding activity has 5′-to-3′ polarity. This finding implies that the coronavirus helicase binds to the 5′ single-stranded region of a partial-duplex RNA and unwinds this duplex in a 5′-to-3′ direction with respect to the RNA strand used for entry. In this context, it will be important to find out whether the difference in the polarity of the unwinding process between the coronavirus helicase and RNA viral SF2 helicases also reflects a fundamental difference between SF1 and SF2 helicases, that is, do other RNA viral SF1 helicases share the 5′-to-3′ polarity with the coronavirus helicase. The only other RNA viral SF1 helicase activity reported so far, that of the Semliki Forest virus nsp2 protein, showed extremely low duplex-unwinding activity in vitro and, to our knowledge, has not yet been characterized with regard to its polarity (Gomez de Cedrón et al., 1999).

Studies on molecular motors of the kinesin superfamily (Henningsen & Schliwa, 1997) have demonstrated that the specific arrangement of motor domains with their associated accessory domains may determine the polarity of translocation. It is therefore con-

https://doi.org/10.1017/S1355838200000728 Published online by Cambridge University Press

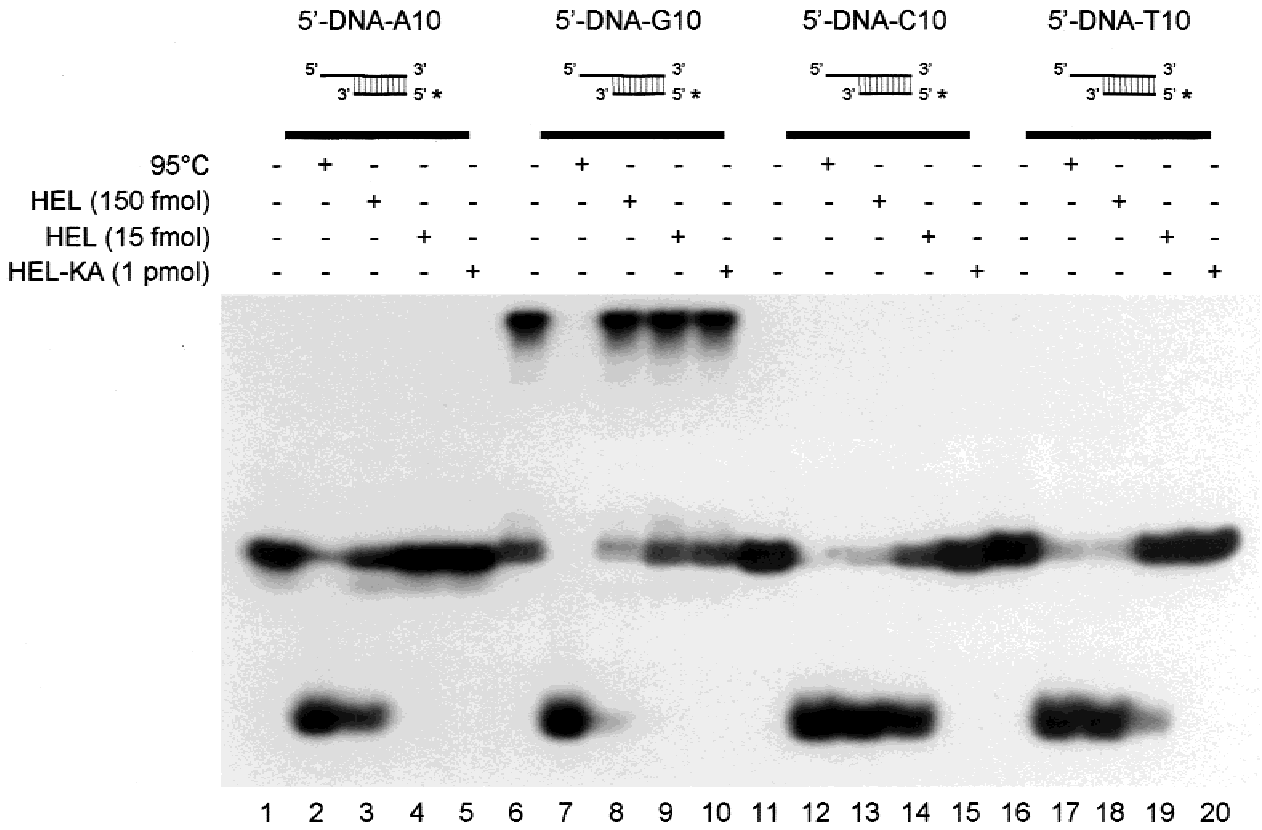

FIGURE 6. The effect of 5′-tail nucleotide composition on DNA duplex unwinding activity of HEL. Reactions were done as described in Materials and methods with approximately 25 fmol of DNA substrate per reaction and analyzed on 10–20% gradient polyacrylamide gels. The DNA substrates were composed of identical 22-bp duplex regions and 10-nt-long 5′ single-stranded tails of oligo(dA) (lanes 1–5), oligo(dG) (lanes 6–10), oligo(dC) (lanes 11–15) or oligo(dT) (lanes 16–20). Asterisks indicate radiolabeled strands. Lanes 1, 6, 11, and 16: reactions without protein; lanes 2, 7, 12, and 17: heat-denatured DNA substrate; lanes 3, 8, 13, and 18: reactions containing 150 fmol HEL; lanes 4, 9, 14, and 19: reactions containing 15 fmol HEL; lanes 5, 10, 15, and 20: reactions containing 1 pmol HEL-KA.

ceivable that the directionality of helicases may also be controlled by additional domains rather than by the intrinsic properties of the core helicase itself. Indeed, numerous cellular helicases carry additional nucleic acid-binding domains, including zinc finger structures (reviewed in Gorbalenya & Koonin, 1993). Most of these additional domains are either attached to one or the other of the core helicase termini, or they are inserted between the helicase motifs Ia and II or IV and V, respectively (Gorbalenya & Koonin, 1993; Bird et al., 1998). Obviously, it will be interesting to examine if the amino terminal zinc finger contributes to the function of the coronavirus helicase. Furthermore, the possibility that there are additional contacts between the HCoV enzyme and the duplex region of the substrate needs to be investigated. Such interactions have recently been postulated to be of critical importance for the duplex-unwinding activity of the bacterial DNA helicase PcrA (Velankar et al., 1999).

Another important finding of this study is the apparent lack of specificity of the coronavirus helicase for RNA versus DNA substrates. The vast majority of helicases act in a very specific manner on either RNA or DNA. The few enzymes that lack this specificity (Stahl et al., 1986; Scheffner et al., 1989; Zhang & Grosse, 1994; Bayliss & Smith, 1996; Gwack et al., 1997; Laxton et al., 1998; Costa et al., 1999; Kim et al., 1999) are mainly virus encoded or so-called noncanonical helicases. Structural data on one of these enzymes, HCV NS3, have recently shown that the primary interactions between NS3 and the single-stranded substrate are directed to the phosphate backbone and not the base or ribose of the substrate, which may explain the apparent lack of substrate specificity of NS3 (Kim et al., 1998).

The conclusion that the nucleic acid-binding pocket of the recombinant HCoV helicase, the HEL protein, does not discriminate significantly between DNA and RNA is further supported by the strong stimulation of the HEL-associated ATPase activity by both polynucleotides and polyribonucleotides. This property is also found in some cellular helicases (Lee & Hurwitz, 1993; Czaplinski et al., 1995) and other viral helicases (Suzich et al., 1993; Gross & Shuman, 1995; Preugschat et al., 1996). The extent of ATPase activity stimulation by nucleic acids was surprisingly high and, in some

https://doi.org/10.1017/S1355838200000728 Published online by Cambridge University Press

cases, even surpassed the values reported for viral SF2 helicases (Preugschat et al., 1996). On the basis of structural data, it has recently been suggested that the binding of single-stranded DNA induces conformational changes in the protein, which, in turn, stabilizes the bound ATP molecule in a conformation that is required for rapid hydrolysis (Soultanas et al., 1999). It is therefore reasonable to suggest that the observed stimulatory effect of nucleic acids on the coronavirus ATPase activity may reflect similar conformational changes. The fact that poly(dA) was more stimulatory than its ribonucleic acid counterpart, poly(A), was surprising for an enzyme presumably involved in RNA metabolism, but it is not unprecedented in RNA virus helicases (Preugschat et al., 1996).

Biological role of the HCoV helicase activity

The data described here do not allow for definitive conclusions concerning the function of a 5′-to-3′ helicase activity in coronavirus replication and transcription. However, because double-stranded replicative intermediates are believed to be the predominant RNA structures in coronaviral RNA synthesis (for a review, see van der Most & Spaan, 1995), it is tempting to speculate that, in analogy to models described for the replisome (reviewed in Baker & Bell, 1998), the coronavirus helicase operates in conjunction with RdRp and, by translocating along the "lagging strand" RNA template, provides the single-stranded RNA template for processive ("leading strand") RNA synthesis. It is noteworthy that the vaccinia virus NPH-II RNA helicase has recently been shown to be a highly processive enzyme that unwinds long duplex RNA structures (Jankowsky et al., 2000). This data contradicts the previously held belief that processivity can only be attributed to DNA helicases (de la Cruz et al., 1999) and supports the hypothesis that, at least some viral RNA helicases might be "replicative" helicases in the true sense.

Because coronaviruses are RNA viruses that replicate in the cytoplasm of the infected cell, it appears unlikely that the HEL DNA helicase activity has any relevance to a specific function in viral RNA synthesis. However, as illustrated for the HCV NS3 helicase, the in vitro DNA helicase activity greatly facilitates biochemical and structural analyses (Preugschat et al., 1996; Korolev et al., 1997; Kim et al., 1998). We have used the DNA helicase activity of HEL to investigate the effects of length and sequence variations in the 5′ tail of a partial-duplex DNA substrate on duplex unwinding. The data we have obtained do not allow us to propose a well-defined sequence specificity of the coronavirus helicase, as has been possible for other proteins (Fuller-Pace et al., 1993; Nicol & Fuller-Pace, 1995; O'Day et al., 1996; Xu et al., 1996), but they are a first step in the identification of biologically relevant, coronavirus-specific helicase substrates.

The HCoV replicase polyprotein 1ab of which the helicase domain is part has a molecular mass of about 750 kDa. This primary translation product is extensively processed into more than 15 mature proteins by viral proteinases (reviewed in Ziebuhr et al., 2000), and it is believed that both the replication of the coronavirus genome and the transcription of the nested set of 3′-coterminal mRNAs involve processes whose complexity goes far beyond that seen in other (+) RNA viruses. Because of the unparalleled size of the coronavirus RNA genome (about 30 kb), genetic approaches to the analysis of replicase gene function have been limited to date. Thus, the biochemical approach has proven to be the most valuable source of information in the study of the coronaviral replicative proteins. We believe that the recombinant form of the HCoV helicase can be used for comprehensive biochemical and, possibly, structural analyses that can be expected to provide insights into the functions of this enzyme in the viral life-cycle.

MATERIALS AND METHODS

Construction of baculovirus recombinants

The coding sequence of the HCoV pp1ab amino acids 4998–5592 was amplified by PCR from plasmid pBS-T13A5 DNA (Herold et al., 1993) using the oligonucleotides 5′-TTTTAGATCTTGGTCTTTGTGTAGTATGTGGTTCTC-3′ and 5′-AACTGCAGTTACTGTAAATCTGTCATAGTGA-3′. The upstream primer contained a *Bgl*II restriction site and the downstream primer contained a translation stop codon, preceding a *Pst*I restriction site. The PCR product was digested with *Bgl*II and *Pst*I and ligated with the larger fragment of *Bam*HI/*Pst*I-digested pBlueBacHis2B DNA (Invitrogen; Groningen, Netherlands). The resultant plasmid, pBlueBacHis2B-Hel, encodes a protein that comprises 32 vector-derived, amino-terminal amino acids (including 6 consecutive His residues and an enterokinase cleavage site) and the HCoV helicase. As a result of the cloning strategy, the two amino-terminal Ala residues of the HCoV helicase (pp1ab amino acids 4996 and 4997) were substituted by Asp and Leu, respectively.

A recombination-PCR method (Yao et al., 1992) was used to introduce a point mutation into the helicase-coding sequence of pBlueBacHis2B-Hel. In the resultant plasmid, pBlueBacHis2B-HEL-KA, the codon for the HCoV pp1ab amino acid Lys-5284, AAA, was substituted by GCA, which encodes Ala.

The plasmids pBlueBacHis2B-Hel and pBlueBacHis2B-HEL-KA were used to derive two recombinant baculoviruses, designated vBac-Hel and vBac-HEL-KA, respectively. Insect *Sf*9 cells and the Bac-N-Blue™ transfection kit were purchased from Invitrogen. Cell culture, transfections, isolation of recombinant baculoviruses, and plaque purification were done as recommended by the manufacturer.

Protein expression and purification

High Five™ insect cells (Invitrogen) were infected with recombinant baculovirus at a multiplicity of infection of five. At

https://doi.org/10.1017/S1355838200000728 Published online by Cambridge University Press

48 h postinfection, the cells were pelleted, washed twice with phosphate-buffered saline (PBS), and resuspended in buffer A (20 mM sodium phosphate, pH 7.0, 1 M NaCl, 10% (v/v) glycerol, 2 mM β-mercaptoethanol, 25 mM imidazol; 1.25 mL per 10^7 cells) containing 10 μM leupeptin. All subsequent purification steps were done at 4 °C. The cells were lysed by two cycles of freezing/thawing and DNA was sheared by passing the cell lysate four times through an 18-gauge needle. The cell debris was pelleted by centrifugation at 27,000 × *g* for 30 min and the supernatant was incubated with 200 μL ProBond™ resin (Invitrogen) that had been preequilibrated with buffer B (buffer A containing 0.1% (v/v) Tween 20). After 2 h, the resin was pelleted and nonspecifically bound proteins were removed by two washes in buffer B, followed by three washes in buffer C (20 mM sodium phosphate, pH 6.0, 1 M NaCl, 10% (v/v) glycerol, 2 mM β-mercaptoethanol, 0.1% (v/v) Tween 20) containing 25 mM, 50 mM, and 100 mM imidazole, respectively. The recombinant His-tagged protein was eluted with buffer C containing 500 mM imidazole. The protein solution was then extensively dialyzed with buffer D (20 mM sodium phosphate, pH 7.4, 200 mM NaCl, 10% (v/v) glycerol, 1 mM dithiothreitol). Next, $CaCl_2$ was added to a concentration of 1 mM and the solution was incubated for 16 h in the presence of 500 U nuclease S7 (Boehringer Mannheim; Mannheim, Germany). Finally, the proteins were again purified by ProBond™ affinity chromatography as described above and dialyzed with buffer D. Dithiothreitol was added to a concentration of 5 mM, and the purified His-tagged proteins, HEL and HEL-KA, were stored at −80 °C.

SDS-polyacrylamide gel electrophoresis and western blotting were done using standard techniques (Sambrook et al., 1989). The partially purified mouse monoclonal antibody 6.2E11 (U. Harms, unpubl.), which specifically recognizes HCoV pp1ab amino acids 5104–5122, was generously provided by U. Harms.

Preparation of duplex RNA and DNA substrates

3′-RNA1

Plasmid pBluescript II KS(+) DNA (Stratagene, La Jolla, California) was digested with *Sac*I and *Kpn*I and treated with T4 DNA polymerase and the large fragment was religated using T4 DNA ligase. The resultant plasmid was linearized with *Pvu*II and used as the template for run-off transcription with either T7 RNA polymerase or T3 RNA polymerase. The T3 transcript was synthesized in the presence of 2 μCi/μL [α-^{32}P]-CTP (800 Ci/mmol).

5′-RNA1

Plasmid pBST-Hel was produced by the insertion of DNA encoding HCoV pp1ab amino acids 4996–5592 into the *Bam*HI/*Sal*I sites of plasmid pBST (Grötzinger et al., 1996). pBST-Hel DNA was digested with *Nde*I and *Kpn*I, treated with T4 DNA polymerase, and religated. The resultant plasmid was linearized with either *Dra*III or *Aci*I and used as the template for run-off transcription with either T7 RNA polymerase or T3 RNA polymerase. The T3 transcript was synthesized in the presence of 2 μCi/μL [α-^{32}P]-CTP (800 Ci/mmol).

3′-RNA2

Two synthetic oligonucleotides, 3′-R2a (5′-CACTCCC-d$(pT)_{15}$-AAA-3′) and 3′-R2b (5′-TTT-d$(pA)_{15}$-GGGAGTGAGCT-3′), were annealed, phosphorylated with T4 polynucleotide kinase, and ligated with the larger fragment of *Sac*I/*Eco*RV-digested pBluescript II KS(+) DNA. The resultant plasmid was linearized with *Dra*I and used as the template for run-off transcription with T7 RNA polymerase. For the preparation of the partially complementary RNA strand, two oligonucleotides, 3′–R2c (5′-CGCGCGTAATACGACTCACTATAGGG AGTGAGCTCCAATTCGCCCGGG-3′) and 3′-R2d (5′-CG CGCCCGGGCGAATTGGAGCTCACTCCCTATAGTGAGTCG TATTACG-3′) were annealed, phosphorylated, and ligated with the larger fragment of *Bss*HII-digested pBluescript II KS(+) DNA. The resultant plasmid was linearized with *Sma*I and used as the template for run-off transcription with T7 RNA polymerase in the presence of 2 μCi/μL [α-^{32}P]-CTP (800 Ci/mmol).

5′-RNA2

Two oligonucleotides, 5′-R2a (5′-CGTTGGCGCGCTAATAC GACTCACTATAGGGATCCCTTTAGTGAGGGTTAATTGCGC GCGTTGC-3′), and 5′-R2b (5′-GCAACGCGCGCAATTAA CCCTCACTAAAGGGATCCCTATAGTGAGTCGTATTAGCGC GCCAACG-3′) were annealed, digested with *Bss*HII, and ligated with the large fragment of *Bss*HII-digested pBluescript II KS(+) DNA. The resultant plasmid was designated pBS-65/66. Next, two oligonucleotides 5′-R2c (5′-GATC-d$(pT)_{15}$-CTAGAACCGCTGCGGCTGGATCCCG-3′) and 5′-R2d (5′-CGGGATCCAGCCGCAGCGGTTCTAG-d$(pA)_{15}$-GATC-3′) were annealed, digested with *Bam*HI, and ligated with *Bam*HI-digested pBS-65/66. The resultant plasmid was linearized with either *Bam*HI or *Xba*I and used as a template for run-off transcription with either T7 RNA Polymerase or T3 RNA polymerase. The T3 transcript was synthesized in the presence of 2 μCi/μL [α-^{32}P]-CTP (800 Ci/mmol).

In vitro-transcribed RNA was purified by phenol/chloroform extraction and gel filtration chromatography using Micro Bio-Spin 6 Columns (Bio-Rad Laboratories; Munich, Germany). The RNA duplex was produced by annealing a mixture of two RNAs with a 10-fold excess of unlabeled RNA over [α-^{32}P]-CTP-labeled RNA in buffer E (25 mM HEPES-KOH, pH 7.4, 500 mM NaCl, 1 mM EDTA, 0.1% (w/v) SDS). The reaction mixture was denatured for 5 min at 95 °C and slowly cooled to room temperature.

To produce duplex DNA substrates, two synthetic oligonucleotides (HPSF-quality, MWG-Biotech; Munich, Germany) were annealed as described above. Oligonucleotides were labeled with [γ-^{32}P]-ATP (3,000 Ci/mmol) using T4 polynucleotide kinase. The labeled DNA was purified by phenol/chloroform extraction and gel filtration chromatography using Micro Bio-Spin 6 columns.

DNA–0

The radioactively labeled oligonucleotide DR (5′-GGTGCA GCCGCAGCGGTGCTCG-3′) and oligonucleotide D1 (5′-CG AGCACCGCTGCGGCTGCACC-3′) were annealed. This substrate contained no single-stranded regions.

https://doi.org/10.1017/S1355838200000728 Published online by Cambridge University Press

5′-3′-DNA-T30

The radioactively labeled oligonucleotide D2 (5′-GGTGC AGCCGCAGCGGTGCTCG-d(pT)$_{30}$-3′) and oligonucleotide D3 (5′-d(pT)$_{30}$-CGAGCACCGCTGCGGCTGCACC-3′) were annealed. This twin-tailed ("forked") substrate contained 5′ and 3′ single-stranded regions on one end of the partial duplex DNA.

5′-DNA-3′-T30

The radioactive labeled oligonucleotide DR and oligonucleotide D4 (5′-d(pT)$_{30}$-CGAGCACCGCTGCGGCTGCACC-d(pT)$_{30}$-3′) were annealed. This substrate contained 5′ and 3′ single-stranded regions at opposite ends of the partial duplex DNA.

3′-DNA-T30

The oligonucleotide D1 and the radioactively labeled oligonucleotide D2 were annealed.

5′-DNA-T30

The radioactively labeled oligonucleotide DR and oligonucleotide D3 were annealed.

5′-DNA-T20

The radioactively labeled oligonucleotide DR and oligonucleotide D5 (5′-d(pT)$_{20}$-CGAGCACCGCTGCGGCTGCACC-3′) were annealed.

5′-DNA-T10

The radioactively labeled oligonucleotide DR and oligonucleotide D6 (5′-d(pT)$_{10}$-CGAGCACCGCTGCGGCTGCACC-3′) were annealed.

5′-DNA-T5

The radioactively labeled oligonucleotide DR and oligonucleotide D7 (5′-d(pT)$_5$-CGAGCACCGCTGCGGCTGCACC-3′) were annealed.

5′-DNA-A10

The radioactively labeled oligonucleotide DR and oligonucleotide D8 (5′-d(A)$_{10}$-CGAGCACCGCTGCGGCTGCACC-3′) were annealed.

5′-DNA-G10

The radioactively labeled oligonucleotide DR and oligonucleotide D9 (5′-d(G)$_{10}$-CGAGCACCGCTGCGGCTGCACC-3′) were annealed.

5′-DNA-C10

The radioactively labeled oligonucleotide DR and oligonucleotide D10 (5′-d(C)$_{10}$-CGAGCACCGCTGCGGCTGCACC-3′) were annealed.

Duplex-unwinding assay

HEL or HEL-KA was incubated in a volume of 40 μL with 25–90 fmol partial-duplex RNA or DNA substrates for 30 min at 30 °C in a buffer containing 20 mM HEPES-KOH, pH 7.4, 5 mM ATP, 10% glycerol, 5 mM magnesium acetate, 2 mM dithiothreitol, and 0.1 mg/mL bovine serum albumin. The NaCl concentration in the reactions, resulting from substrate and protein storage buffers, was 37.5 mM. The reactions were stopped by the addition of 10 μL of 5% (v/v) SDS, 15% (w/v) Ficoll, and 100 mM EDTA. The reaction products were separated on 6%, 12%, or 10–20% gradient polyacrylamide-1× TBE gels (acrylamide/bis-acrylamide ratio of 19:1) at 4 W until the bromphenol blue dye approached the bottom of the gel. The gels were exposed to X-ray film at −70 °C.

Nucleoside triphosphatase assay

In the ATPase assay, HEL (30 fmol) or HEL-KA (210 fmol) was incubated in a volume of 40 μL containing 20 mM HEPES-KOH, pH 7.4, 300 μM ATP, 5 mM magnesium acetate, 2 mM dithiothreitol, 25 μg/mL bovine serum albumin, and 250 nCi of [γ-^{32}P]-ATP (3,000 Ci/mmol). In the GTPase assay, ATP and [γ-^{32}P]-ATP were replaced by 300 μM GTP and 250 nCi [γ-^{32}P]-GTP (3,000 Ci/mmol), respectively. When included, polynucleotides and polyribonucleotides (5.4–8.3 Svedberg units) were at a concentration of 50 μg/mL. The reactions were incubated at 30 °C for 30 min and stopped by adding EDTA to a final concentration of 100 mM. The samples were analyzed by polyethyleneimine-cellulose thin layer chromatography with 0.15 M formic acid-0.15 M LiCl (pH 3.0) as the liquid phase. The reaction products were quantitated by phosphorimaging of the dried chromatographic plates (ImageQuant software; Molecular Dynamics, Sunnyvale, California).

ACKNOWLEDGMENTS

The authors would like to thank U. Harms for the antibody 6.11.E2. We are also grateful to A.E. Gorbalenya for suggestions for this manuscript. This work was supported by grants from the Deutsche Forschungsgemeinschaft (SI 357/4-1, GK Infektiologie) and the Fonds der chemischen Industrie (FCI).

Received March 30, 2000; returned for revision
April 24, 2000; revised manuscript received May 4, 2000

REFERENCES

Baker TA, Bell SP. 1998. Polymerases and the replisome: Machines with machines. *Cell 92*:295–305.

Bayliss CD, Smith GL. 1996. Vaccinia virion protein I8R has both DNA and RNA helicase activities: Implications for vaccinia virus transcription. *J Virol 70*:794–800.

Bird LE, Subramanya HS, Wigley DB. 1998. Helicases: A unifying structural theme? *Curr Opin Struct Biol 8*:14–18.

Buck KW. 1996. Comparison of the replication of positive-stranded RNA viruses of plants and animals. *Adv Virus Res 47*:159–251.
Cho HS, Ha NC, Kang LW, Chung KM, Back SH, Jang SK, Oh BH. 1998. Crystal structure of RNA helicase from genotype 1b hepatitis C virus. A feasible mechanism of unwinding duplex RNA. *J Biol Chem 273*:15045–15052.
Costa M, Ochem A, Staub A, Falaschi A. 1999. Human DNA helicase VIII: A DNA and RNA helicase corresponding to the G3BP protein, an element of the ras transduction pathway. *Nucleic Acids Res 27*:817–821.
Czaplinski K, Wenig Y, Hagan KW, Peltz SW. 1995. Purification and characterization of the Upf1 protein: A factor involved in translation and mRNA degradation. *RNA 1*:610–623.
Dé I, Sawicki SG, Sawicki DL. 1996. Sindbis virus RNA-negative mutants that fail to convert from minus-strand to plus-strand synthesis: Role of the nsP2 protein. *J Virol 70*:2706–2719.
de la Cruz J, Kressler D, Linder P. 1999. Unwinding RNA in *Saccharomyces cerevisiae*: DEAD-box proteins and related families. *Trends Biochem Sci 24*:192–198.
den Boon JA, Snijder EJ, Chirnside ED, de Vries AA, Horzinek MC, Spaan WJM. 1991. Equine arteritis virus is not a togavirus but belongs to the coronaviruslike superfamily. *J Virol 65*:2910–2920.
Fuller-Pace FV, Nicol SM, Reid AD, Lane DP. 1993. DbpA: A DEAD box protein specifically activated by 23S rRNA. *EMBO J 12*:3619–3626.
Gomez de Cedrón M, Ehsani N, Mikkola ML, García JA, Kääriäinen L. 1999. RNA helicase activity of Semliki Forest virus replicase protein NSP2. *FEBS Lett 448*:19–22.
Gorbalenya AE, Koonin EV. 1989. Viral proteins containing the purine NTP-binding sequence pattern. *Nucleic Acids Res 17*:8413–8440.
Gorbalenya AE, Koonin EV. 1993. Helicases: Amino acid sequence comparisons and structure-function relationships. *Curr Opin Struct Biol 3*:419–429.
Gorbalenya AE, Koonin EV, Donchenko AP, Blinov VM. 1989a. Coronavirus genome: Prediction of putative functional domains in the non-structural polyprotein by comparative amino acid sequence analysis. *Nucleic Acids Res 17*:4847–4861.
Gorbalenya AE, Koonin EV, Donchenko AP, Blinov VM. 1989b. Two related superfamilies of putative helicases involved in replication, recombination, repair and expression of DNA and RNA genomes. *Nucleic Acids Res 17*:4713–4730.
Gros C, Wengler G. 1996. Identification of an RNA-stimulated NTPase in the predicted helicase sequence of the Rubella virus nonstructural polyprotein. *Virology 217*:367–372.
Gross CH, Shuman S. 1995. Mutational analysis of vaccinia virus nucleoside triphosphate phosphohydrolase II, a DExH box RNA helicase. *J Virol 69*:4727–4736.
Grötzinger C, Heusipp G, Ziebuhr J, Harms U, Süss J, Siddell SG. 1996. Characterization of a 105-kDa polypeptide encoded in gene 1 of the human coronavirus HCV 229E. *Virology 222*:227–235.
Gwack Y, Kim DW, Han JH, Choe J. 1997. DNA helicase activity of the hepatitis C virus nonstructural protein 3. *Eur J Biochem 250*:47–54.
Hall MC, Matson SW. 1999. Helicase motifs: The engine that powers DNA unwinding. *Mol Microbiol 34*:867–877.
Henningsen U, Schliwa M. 1997. Reversal in the direction of movement of a molecular motor. *Nature 389*:93–96.
Herold J, Raabe T, Schelle-Prinz B, Siddell SG. 1993. Nucleotide sequence of the human coronavirus 229E RNA polymerase locus. *Virology 195*:680–691.
Heusipp G, Harms U, Siddell SG, Ziebuhr J. 1997. Identification of an ATPase activity associated with a 71-kilodalton polypeptide encoded in gene 1 of the human coronavirus 229E. *J Virol 71*:5631–5634.
Janda M, Ahlquist P. 1998. Brome mosaic virus RNA replication protein 1a dramatically increases in vivo stability but not translation of viral genomic RNA3. *Proc Natl Acad Sci USA 95*:2227–2232.
Jankowsky E, Gross CH, Shuman S, Pyle AM. 2000. The DExH protein NPH-II is a processive and directional motor for unwinding RNA. *Nature 403*:447–451.
Kadaré G, David C, Haenni, AL. 1996. ATPase, GTPase, and RNA binding activities associated with the 206-kilodalton protein of turnip yellow mosaic virus. *J Virol 70*:8169–8174.
Kadaré G, Haenni AL. 1997. Virus-encoded RNA helicases. *J Virol 71*:2583–2590.
Kim HD, Choe J, Seo YS. 1999. The sen1(+) gene of *Schizosaccharomyces pombe*, a homologue of budding yeast SEN1, encodes an RNA and DNA helicase. *Biochemistry 38*:14697–14710.
Kim JL, Morgenstern KA, Griffith JP, Dwyer MD, Thomson JA, Murcko MA, Lin C, Caron PR. 1998. Hepatitis C virus NS3 RNA helicase domain with a bound oligonucleotide: The crystal structure provides insights into the mode of unwinding. *Structure 6*:89–100.
Koonin EV, Dolja VV. 1993. Evolution and taxonomy of positive-strand RNA viruses: Implications of comparative analysis of amino acid sequences. *Crit Rev Biochem Mol Biol 28*:375–430.
Korolev S, Hsieh J, Gauss GH, Lohman TM, Waksman G. 1997. Major domain swiveling revealed by the crystal structures of complexes of *E. coli* Rep helicase bound to single-stranded DNA and ADP. *Cell 90*:635–647.
Korolev S, Yao N, Lohman TM, Weber PC, Waksman G. 1998. Comparisons between the structures of HCV and Rep helicases reveal structural similarities between SF1 and SF2 super-families of helicases. *Protein Sci 7*:605–610.
Kroner PA, Young BM, Ahlquist P. 1990. Analysis of the role of brome mosaic virus 1a protein domains in RNA replication, using linker insertion mutagenesis. *J Virol 64*:6110–6120.
Kwong AD, Kim JL, Lin C. 2000. Structure and function of hepatitis C virus NS3 helicase. *Curr Top Microbiol Immunol 242*:171–196.
Laxton CD, McMillan D, Sullivan V, Ackrill AM. 1998. Expression and characterization of the hepatitis G virus helicase. *J Viral Hepat 5*:21–26.
Lee CG, Hurwitz J. 1993. Human RNA helicase A is homologous to the maleless protein of *Drosophila*. *J Biol Chem 268*:16822–16830.
Linder P, Daugeron MC. 2000. Are DEAD-box proteins becoming respectable helicases? *Nat Struct Biol 7*:97–99.
Lohman TM, Bjornson KP. 1996. Mechanisms of helicase-catalyzed DNA unwinding. *Annu Rev Biochem 65*:169–214.
Nicol SM, Fuller-Pace FV. 1995. The "DEAD box" protein DbpA interacts specifically with the peptidyltransferase center in 23S rRNA. *Proc Natl Acad Sci USA 92*:11681–11685.
O'Day CL, Chavanikamannil F, Abelson J. 1996. 18S rRNA processing requires the RNA helicase-like protein Rrp3. *Nucleic Acids Res 24*:3201–3207.
O'Reilly EK, Tang N, Ahlquist P, Kao CC. 1995. Biochemical and genetic analyses of the interaction between the helicase-like and polymerase-like proteins of the brome mosaic virus. *Virology 214*:59–71.
O'Reilly EK, Wang Z, French R, Kao CC. 1998. Interactions between the structural domains of the RNA replication proteins of plant-infecting RNA viruses. *J Virol 72*:7160–7169.
Osman TA, Buck KW. 1996. Complete replication in vitro of tobacco mosaic virus RNA by a template-dependent, membrane-bound RNA polymerase. *J Virol 70*:6227–6234.
Petty IT, French R, Jones RW, Jackson AO. 1990. Identification of barley stripe mosaic virus genes involved in viral RNA replication and systemic movement. *EMBO J 9*:3453–3457.
Pfister T, Wimmer E. 1999. Characterization of the nucleoside triphosphatase activity of poliovirus protein 2C reveals a mechanism by which guanidine inhibits poliovirus replication. *J Biol Chem 274*:6992–7001.
Phillips K, Dauter Z, Murchie AI, Lilley DM, Luisi B. 1997. The crystal structure of a parallel-stranded guanine tetraplex at 0.95 Å resolution. *J Mol Biol 273*:171–182.
Preugschat F, Averett DR, Clarke BE, Porter DJT. 1996. A steady-state and pre-steady-state kinetic analysis of the NTPase activity associated with the hepatitis C virus NS3 helicase domain. *J Biol Chem 271*:24449–24457.
Rikkonen M, Peränen J, Kääriäinen L. 1994. ATPase and GTPase activities associated with Semliki Forest virus nonstructural protein nsP2. *J Virol 68*:5804–5810.
Rodriguez PL, Carrasco L. 1993. Poliovirus protein 2C has ATPase and GTPase activities. *J Biol Chem 268*:8105–8110.
Rouleau M, Smith RJ, Bancroft JB, Mackie, GA. 1994. Purification, properties, and subcellular localization of foxtail mosaic potexvirus 26-kDa protein. *Virology 204*:254–265.
Sambrook J, Fritsch EF, Maniatis T. 1989. *Molecular cloning: A laboratory manual*, 2nd ed. Cold Spring Harbor, New York: Cold Spring Harbor Laboratory Press.

https://doi.org/10.1017/S1355838200000728 Published online by Cambridge University Press

Scheffner M, Knippers R, Stahl H. 1989. RNA unwinding activity of SV40 large T antigen. *Cell 57*:955–963.
Schmid SR, Linder P. 1992. D-E-A-D protein family of putative RNA helicases. *Mol Microbiol 6*:283–291.
Soultanas P, Dillingham MS, Velankar SS, Wigley DB. 1999. DNA binding mediates conformational changes and metal ion coordination in the active site of PcrA helicase. *J Mol Biol 290*:137–148.
Stahl H, Droge P, Knippers R. 1986. DNA helicase activity of SV40 large tumor antigen. *EMBO J 5*:1939–1944.
Subramanya HS, Bird LE, Brannigan JA, Wigley DB. 1996. Crystal structure of a DExx box DNA helicase. *Nature 384*:379–383.
Suzich JA, Tamura JK, Palmer-Hill F, Warrener P, Grakoui A, Rice CM, Feinstone SM, Collett MS. 1993. Hepatitis C virus NS3 protein polynucleotide-stimulated nucleoside triphosphatase and comparison with the related pestivirus and flavivirus enzymes. *J Virol 67*:6152–6158.
van der Most RG, Spaan WJM. 1995. Coronavirus replication, transcription, and RNA recombination. In: Siddell SG, ed. *The Coronaviridae*. New York: Plenum Press. pp 11–31.
van Dinten LC, den Boon JA, Wassenaar AL, Spaan WJ, Snijder EJ. 1997. An infectious arterivirus cDNA clone: Identification of a replicase point mutation that abolishes discontinuous mRNA transcription. *Proc Natl Acad Sci USA 94*:991–996.
van Dinten LC, Rensen S, Gorbalenya AE, Snijder EJ. 1999. Proteolytic processing of the open reading frame 1b-encoded part of arterivirus replicase is mediated by nsp4 serine protease and is essential for virus replication. *J Virol 73*:2027–2037.
van Dinten LC, Wassenaar AL, Gorbalenya AE, Spaan WJ, Snijder, EJ. 1996. Processing of the equine arteritis virus replicase ORF1b protein: Identification of cleavage products containing the putative viral polymerase and helicase domains. *J Virol 70*:6625–6633.
Velankar SS, Soultanas P, Dillingham MS, Subramanya HS, Wigley DB. 1999. Crystal structures of complexes of PcrA DNA helicase with a DNA substrate indicate an inchworm mechanism. *Cell 97*:75–84.
Walker JE, Saraste M, Runswick MJ, Gay NJ. 1982. Distantly related sequences in the alpha- and beta-subunits of ATP synthase, myosin, kinases and other ATP-requiring enzymes and a common nucleotide binding fold. *EMBO J 1*:945–951.
Xu D, Nouraini S, Field D, Tang SJ, Friesen JD. 1996. An RNA-dependent ATPase associated with U2/U6 snRNAs in pre-mRNA splicing. *Nature 381*:709–713.
Yao N, Hesson T, Cable M, Hong Z, Kwong AD, Le HV, Weber PC. 1997. Structure of the hepatitis C virus RNA helicase domain. *Nat Struct Biol 4*:463–467.
Yao Z, Jones DH, Grose C. 1992. Site-directed mutagenesis of herpesvirus glycoprotein phosphorylation sites by recombination polymerase chain reaction. *PCR Methods Appl 1*:205–207.
Zhang S, Grosse F. 1994. Nuclear DNA helicase II unwinds both DNA and RNA. *Biochemistry 33*:3906–3912.
Ziebuhr J, Herold J, Siddell SG. 1995. Characterization of a human coronavirus (strain 229E) 3C-like proteinase activity. *J Virol 69*:4331–4338.
Ziebuhr J, Snijder EJ, Gorbalenya AE. 2000. Virus-encoded proteinases and proteolytic processing in the *Nidovirales*. *J Gen Virol 81*:853–879.

https://doi.org/10.1017/S1355838200000728 Published online by Cambridge University Press